Journal of Helminthology

cambridge.org/jhl

Research Paper

Cite this article: Amin OM, Chaudhary A, Singh HS (2022). New perspectives of *Microsentis wardae* Martin & Multani, 1966 (Acanthocephala: Neoechinorhynchidae) from *Gillichthys mirabilis* Cooper in California, with scanning electron microscopy images and energy dispersive X-ray analysis. *Journal of Helminthology* **96**, e42, 1–12. https://doi.org/10.1017/S0022149X22000347

Received: 26 February 2022
Revised: 13 April 2022
Accepted: 16 May 2022

Key Words:
Acanthocephala; *Microsentis wardae*; *Gillichthys mirabilis*; redescription; new features; molecular profile

Author for correspondence:
O.M. Amin, E-mail: omaramin@aol.com

CAMBRIDGE UNIVERSITY PRESS

New perspectives of *Microsentis wardae* Martin & Multani, 1966 (Acanthocephala: Neoechinorhynchidae) from *Gillichthys mirabilis* Cooper in California, with scanning electron microscopy images and energy dispersive X-ray analysis

O. M. Amin[1], A. Chaudhary[2] and H. S. Singh[2,3]

[1]Institute of Parasitic Diseases, 11445 E. Via Linda 2-419, Scottsdale, Arizona 85259, USA; [2]Molecular Taxonomy Laboratory, Department of Zoology, Chaudhary Charan Singh University, Meerut, Uttar Pradesh, 250004, India and [3]Vice Chancellor, Maa Shakumbhari University, Saharanpur, Uttar Pradesh, 247120, India

Abstract

Fully developed, sexually mature small male and female acanthocephalans, *Microsentis wardae* Martin & Multani, 1966 (Neoechinorhynchidae) reaching only 2.25 mm and 2.42 mm, respectively, were collected from the rectum of longjaw mudsuckers, *Gillichthys mirabilis* Cooper, in the salty marches of Anaheim Bay and San Diego Bay, California. Our specimens were half the size of those reported in the original description from the same host in Scammon's Lagoon over 700 km to the south. The ratio of proboscis and receptacle size to trunk size was markedly higher in our specimens compared to the larger specimens measured in the original description. The anatomy of all structures in our specimens from Anaheim Bay was comparable to that of the larger Scammon's Lagoon specimens that have apparently realized more growth in the Scammon's Lagoon. We have observed more structures that are not reported in the original description, especially evident from our scanning electron microscopy images, which are not possible to observe in the original line drawings. In our specimens, the micropores were unusually widely spaced and the energy dispersive X-ray analysis showed longitudinal hook sections with high levels of sulphur and phosphorus and moderate levels of calcium, but the whole hooks showed highest levels of sodium and magnesium – the biochemical hook signature of this species. Sequences of the small subunit (18S) of the nuclear ribosomal DNA were generated and compared with acanthocephalan sequences available from GenBank. As *M. wardae* comprises a monotypic genus, therefore, phylogenetic analyses inferred from the 18S gene showed its relationship with other species of closely related genera of Eoacanthocephala. This is the first report of molecular data of *M. wardae*.

Introduction

Microsentis wardae Martin & Multani, 1966 is one of the smallest and most host and geographically restricted acanthocephalans known to date. It was well described with 12-line drawings from the long-jaw mudsucker *Gillichthys mirabilis* Cooper (Gobiidae) at Scammon's Lagoon in Baja California. It was reported another time since from the same host species and near the same Lagoon in Baja California but not in any of the geographically proximal locations at the Salton Sea, Seal Beach estuaries, Newport Bay and San Francisco Bay by Martin & Multani (1970). The only other report of *M. wardae* was by García-Prieto *et al.* (2010) from the same host species in Laguna Ojo de Liebre (also the same Scammon's Lagoon). This coastal lagoon is located in Mulegé Municipality near the town of Guerrero Negro in the northwestern Baja California Sur state of Mexico. It lies approximately halfway between the southern tip of the Baja California Peninsula and the United States–Mexico border, opening onto the Pacific Ocean (Anonymous, 2009; Phleger & Clifford, 2009). The lagoon is within the Vizcaíno Biosphere Reserve United Nations Educational, Scientific and Cultural Organization World Heritage Site and is a Ramsar wetlands site. This restricted host and geographical distribution of this small acanthocephalan made it less readily accessible for further studies.

A small collection of fully developed adults of *M. wardae*, from the rectum of *G. mirabilis* collected in Anaheim Bay, California have just become available for our study. Anaheim Bay is a wetland salt marsh complex in Orange County about 759 km north of Scammon's Lagoon where *M. wardae* was originally described. These mudsuckers occur in estuaries, primarily in tidal sloughs with shallow mud-covered bottoms, where they often excavate burrows. Their

range extends about 1828 km from Tomales Bay near San Francisco in the north to Bahia Magdalena, Gulf of California, in the south (Eschmeyer *et al.*, 1983; García, 2018). Our present study reports and describes acanthocephalans using scanning electron microscopy (SEM) for the first time and provides new information on its hook biochemistry and molecular biology. The study is the first report to generate molecular data for *M. wardae* and to assess the systematic position of the genus *Microsentis* within Neoechinorhynchidae using molecular data from the 18S nuclear ribosomal gene.

Materials and methods

Collections

Fourteen specimens were collected from the rectum of longjaw mudsuckers, *G. mirabilis* Cooper (Gobiidae) in the salt marshes of Anaheim Bay, California (33.735°N 118.094°W) in December 2017. Twelve specimens were made available. About 30 additional specimens were obtained from 30 examined hosts in Emory Cove Marsh, San Diego Bay (32.6717°N, 117.1441°W) in October 2021. Eight specimens from Anaheim Bay and nine specimens from San Diego Bay were processed for microscopical examination: three for SEM; and five for molecular analysis. The five specimens from Anaheim Bay used for molecular analysis were not properly fixed and were replaced by six specimens from the 2021 San Diego collection.

Deposited material

Specimens were deposited in the University of Nebraska's State Museum's Harold W. Manter Laboratory (HWML) collection, Lincoln, Nebraska.

Methods for microscopical studies

Worms were punctured with a fine needle and subsequently stained in Mayer's acid carmine, destained in 4% hydrochloric acid in 70% ethanol, dehydrated in ascending concentrations of ethanol (24 h each), cleared in 100% xylene and then in Canada balsam xylene in equal proportions (24 h each). Whole worms were then mounted in Canada balsam. Measurements are in micrometres, unless otherwise noted; the range is followed by the mean values in parentheses. Width measurements represent maximum width. Trunk length does not include proboscis, neck, or bursa.

SEM

Specimens that had been fixed and stored in 70% ethanol were processed for SEM following standard methods (Lee, 1992). These included critical point drying and mounting on aluminium SEM sample mounts (stubs) using conductive double-sided carbon tape. The sample was sputter coated with an 80%–20% gold–palladium target for 3 min using a sputter coater (Quorum (Q150T ES) www.quorumtech.com) equipped with a planetary stage, depositing an approximate thickness of 20 nm. The sample was placed and observed in an FEI Helios Dual Beam NanoLab 600 (FEI, Hillsboro, Oregon) scanning electron microscope (FEI, Hillsboro, Oregon). Samples were imaged using an accelerating voltage of 5 kV, and a probe current of 86 pA, at high vacuum using a secondary electron detector.

Focused ion beam (FIB) sectioning of hooks

A dual-beam SEM with gallium ion source (GIS) is used for the liquid ion metal source (LIMS) part of the process. The gallium beam (LIMS) is a gas injection magnetron sputtering technique whereby the rate of cutting can be regulated. The hooks were studied intact and sectioned at two positions (longitudinal sections and cross-sections) using the FEI Helios Dual Beam NanoLab 600 mentioned above. The dual-beam FIB/SEM is equipped with a gallium LIMS. The hooks of the acanthocephalans were centred on the SEM stage and sections were made using an ion accelerating voltage of 30 kV and a probe current of 2.7 nA following the initial cut. The time of cutting is based on the nature and sensitivity of the tissue. The sample also goes through a cleaning cross-section milling process to obtain a smoother surface. The cut was analysed using an X-ray for chemical ions with an electron beam (tungsten) to obtain an X-ray spectrum. The intensity of the GIS was variable according to the nature of the material being cut. Results were stored with the attached imaging software then transferred to a Universal Serial Bus for future use.

Energy dispersive X-ray analysis (EDXA)

The Helios NanoLab 600 is equipped with an EDAX (Mahwah, NJ) TEAM Pegasus system with an Octane Plus detector. The intact hook and the sectioned cuts were analysed by EDXA. Spectra of selected areas were collected from the centre and the edge of each cross-section or longitudinal section. EDXA spectra were collected using an accelerating voltage of 15 kV and a probe current of 1.4 nA. Data collected included images of the displayed spectra as well as the raw collected data. Relative elemental percentages were generated by the TEAM software.

Molecular methods

The DNA extraction from four specimens of *M. wardae* was done using DNeasy® Blood & Tissue Kit (QIAGEN, Hilden, Germany) following the manufacturer's instructions. The 18S region of nuclear ribosomal DNA was amplified by polymerase chain reaction (PCR) using the primer set 18SU467F (forward, 5′-ATCCAAGGAAGGCAGCAGGC-3′) and 18SL1310R (reverse, 5′-CTCCACCAACTAAGAACGGC-3′) (Suzuki *et al.*, 2008). The PCR reactions (25 µl) comprised 3 µl DNA, 2.5 µl of 10× Taq buffer (Biotools, Madrid, Spain), 1 U of Taq polymerase (1 U, Biotools), 3 µl of deoxyribonucleoside triphosphates, 1 µl of each forward and reverse primer and 13.5 µl of deionized water. The amplification reaction was performed with the following cycling parameters: denaturation at 95°C for 3 min for 40 cycles of 94°C for 40 s; 55°C for 45 s; 72°C for 1-min; and termination at 72°C for 10 min. The PCR products were checked on 1% agarose gel and purified with the PureLink™ Quick Gel Extraction and PCR Purification Combo Kit (Invitrogen). Sequencing reactions were done using ABI Big Dye (Applied Biosystems, USA) Terminator vr. 3.1 cycle sequencing kit and detected using an ABI 3130 Genetic Analyzer.

Contigs generated in the present study were assembled using MEGA11 (Tamura *et al.*, 2021). Obtained sequences for the 18S gene of *M. wardae* were aligned with other sequences downloaded from the GenBank database using the Clustal W software (Thompson *et al.*, 1997). 18S sequences were aligned and a nucleotide substitution model was selected using jModelTest version 2.1.7 (Posada, 2008) and the Akaike information criterion

https://doi.org/10.1017/S0022149X22000347 Published online by Cambridge University Press

was applied. For the 18S dataset, the best nucleotide substitution model was GTR + G + I. The phylogenetic tree was reconstructed using the maximum likelihood (ML) method with the software MEGA11 (Tamura *et al.*, 2021) and to assess nodal support 10,000 bootstrap replicates were run. We also estimated phylogenetic relationships using Bayesian inference (BI) in TOPALi 2.5 (Milne *et al.*, 2009), with four independent runs of the Markov chain Monte Carlo chain and posterior probabilities were estimated over 1,000,000 generations with every 100th tree saved and 'Burn-in' was set to 25%. Genetic distances (uncorrected *P*-distance) were estimated with MEGA11.

Results

Morphological observations of our male and female specimens from Anaheim Beach and San Diego Bay, California, were found to be comparable to those described by Martin & Multani (1966) from Scammon's Lagoon over 700 km to the south, with a few variations. The original description included 12 largely accurate and well-presented line drawings. Our specimens, about half the size of those described by Martin & Multani (1966), were also fully developed sexually mature adults found in the rectal area of the same host species, *G. mirabilis*. Table 1 provides a morphometric comparison of the two populations. We opted not to create another set of line drawings that would be repetitious of the detailed ones in the original description. Instead, we have produced a new set of SEM images that depict many features not possible to observe with light microscopy, for the first time, and that elucidate features not described in the Martin & Multani's (1966) text or depicted in the original line drawings. Our treatment will also describe, for the first time, the micropores and the element composition of hooks using EDXA and a molecular profile of the examined specimens.

Description

Microsentis wardae Martin & Multani, 1966

General. Neoechinorhynchidae, with characters of the genus *Microsentis*. Small specimens, with no sexual dimorphism in size and with dorsal and ventral main longitudinal lacunar canals. See table 1 for measurements and counts. Trunk conical, aspinose, widest anteriorly. Neck prominent, widest posteriorly, often bent ventrally. Proboscis large, globular to pear-shaped, about 1/3 size of trunk (figs 1 and 2), with prominent apical organ (fig. 3), sensory pores (fig. 4), nucleated cells, and 16–20 longitudinal rows of 5–6 very small hooks, each. Hooks smallest posteriorly (figs 5–7). All hooks with rectangular roots slightly manubriated anteriorly. Body wall with few scattered electron-dense micropores (fig. 8) and 0–4 dorsal and 0–1 ventral giant hypodermal nuclei. Single-walled receptacle large, about half size of trunk, with cephalic ganglion near its base. Paired lemnisci shorter than receptacle.

Males. Based on 12 sexually mature adults with sperm. See table 1 for measurements and counts. Testes contiguous, always overlapping, at mid-trunk, with anterior testis invariably larger than posterior testis. Sperm duct with prominent elongate sperm vesicles terminating at base of penis. Cement gland large, syncytial, with 5–8 giant nuclei each, connecting posteriorly with almost perfectly spherical cement reservoir opening into penis with 2 ducts. Penis prominent, conical. Saefftigen's pouch elongate, not bulbous anteriorly, invariably at the posterior-most end of trunk on dorsal side. Bursa muscular, without papillae externally (figs 9 and 10).

Females. Based on eight gravid females. Reproductive system somewhat short with relatively small elongate vagina, somewhat large muscular uterus, wide funnel-shaped uterine bell terminally attached to body wall at two different levels and very few basal uterine bell glands. Eggs small elongated ovoid (fig. 11) with slight prolongation of fertilization membrane.

Taxonomic summary

Host. Longjaw mudsuckers, *G. mirabilis* Cooper (Gobiidae).

Localities. The salt marshes of Anaheim Bay, California (33.735°N 118.094°W) and at Emory Cove Marsh, San Diego Bay (32.6717° N, 117.1441° W).

Site of infection. Posterior gut.

Specimens. HWML Helminthological Coll. No. 216779 (voucher specimens on four slides).

Representative DNA sequence. The 18S rDNA sequence of *M. wardae* was deposited in GenBank under the accession numbers OM831948–OM831951.

Remarks

Despite the apparent similarities between our specimens and those described by Martin & Multani (1966) from the same host species in the same intestinal site in California, new and different features became apparent as especially revealed by SEM (figs 1–14) used for the first time. Both populations have included sexually mature adults with sperm and eggs. Table 1 demonstrates that in our specimens, the trunk of both males and females was about half as large as that measured by Martin & Multani (1966) and that the ratio of the size of the proboscis to the size of trunk was considerably larger in our specimens (31–33%) compared to 21–25% in the Martin & Multani (1966) specimens. The same relationship was also observed for the receptacle to trunk ratio (49–44% compared to 30–31%). The extended lemnisci in our specimens were shorter than the receptacle. We added new measurements of the apical organ, the seminal vesicle, the bursa and the diameter of proboscis hooks at base. Our SEM images revealed new features not reported by Martin & Multani (1966) including the ribbed neck, different shaped proboscis, the surface appearance of the apical organ, sensory pores on the proboscis, the elevated proboscis rims at the base of hooks, the widely spaced micropores and the shape of the bursa and the eggs. The line drawings in the original description were detailed, informative and equally applicable to our specimens, the reason for not being repetitious since our SEM images revealed more features not presented by Martin & Multani (1966).

Micropores. The trunk had apparent osmiophilic micropores in most areas – the micropores were more widely spaced compared to the usual less widely distributed micropores more often observed in other acanthocephalan species.

EDXA

The EDXA results of whole hooks and hook sections (table 2) of *M. wardae* show highest level of sulphur and sodium. The EDXA spectra of the mid-hook longitudinal section again show the high-sulphur relative concentration characteristic of the centre core of the mid-hook cross-section as well as the marked concentration of phosphorus. The presence of sulphur, calcium and phosphorus in the EDXA spectra obtained from the hook longitudinal section

https://doi.org/10.1017/S0022149X22000347 Published online by Cambridge University Press

Table 1. Morphometric comparisons between two populations of *Microsentis wardae* from *Gillichthys mirabilis* in California.

	Anaheim Bay, San Diego Bay		Scammon's Lagoon	
	This study		Martin & Multani (1966)	
Character	Males ($n = 12$)	Females ($n = 8$)	Males	Females
trunk length (L) × width (W) (mm)	1.70–2.50 (2.17) × 0.57–0.98 (0.79)[a]	1.57–2.62 (2.06) × 0.65–0.87 (0.75)	up to 4.37 × 1.12	up to 5.00 × 0.69–1.33
giant hypodermal nuclei	0–4 dorsal, 0–1 ventral	0–4 dorsal, 0–1 ventral	4–5 dorsal, 1 ventral	4–5 dorsal, 1 ventral
proboscis L × W	520–850 (681) × 364–625 (477)	550–850 (681) × 375–600 (491)	600–910 × 360–660	730–1260 × 690 × 1330
proboscis L: trunk L	**31%**	**33%**	**21% (maximum numbers)**	**25% (maximum numbers)**
apical organ L × W	**94–198 (160) × 36–94 (71)**[b]	**135–270 (211) × 62–135 (92)**	—	—
hook rows × hooks/row	16–18 (17.6) × 5–7 (5.6)	18–20 (19.0) × 5–7 (5.6)	16–20 × 5–7	17–20 × 6–7
anterior hook L × diameter	15–25 (20) × **3–5 (4.4)**	12–22 (18) × **3–7 (5.0)**	25–43 × —	25–43 × —
middle hook L × diameter	22–26 (24) × **4–6 (5.0)**	20–25 (23) × **5–7 (6.0)**	19–22 × —	19–22 × —
posterior hook L × diameter	14–20 (17) × 2**–6 (3.8)**	10–15 (12) × **3–4 (3.3)**	12 × —	12 × —
neck L × W	208–375 (275) × 270–364 (316)	239–416 (308) × 275–385 (320)	84–560 × 110–420	14–520 × 210–450
receptacle L × W	825–1420 (1070) × 300–625 (460)	750–1125 (914) × 229–475 (325)	770–1330 × 220–420	1040–1540 × 290–530
receptacle L: trunk L	**49%**	**44% (maximum numbers)**	**30% (maximum numbers)**	**31% (maximum numbers)**
lemnisci L × W	**312–900 (582) × 125–250 (162)**	**520–600 (584 × 124–218 (148)**	longer than receptacle (Martin & Multani, 1966, p. 536)	much shorter than receptacle (fig. 8)
anterior testis L × W	364–625 (473) × 260–500 (364)		490–840 × 350–840	
posterior testis L × W	291–550 (396) × 229–400 (344)	—	420–710 × 310–560	—
seminal vesicle L × W	**208–312 (257) × 62–146 (106)**	—	—	—
cement gland L × W	208–500 (360) × 156–395 (277)	—	310–620 × 320–490	—
cement gland giant nuclei	5–8 (6)	—	8	—
cement reservoir L × W	166–260 (200) × 146–239 (184)	—	110–240 × 110–250	—
Saefftigen's pouch L × W	343–541 (458) × 62–135 (104)	—	310–490 × 98–140	—
penis L × W	42–94 (63) × 20–62 (39)	—	70 × 40	—
bursa L × W	**291–498 (404) × 229–312 (282)**	—	—	—
vagina L × W	—	95–156 (129) × 42–95 (57)	—	98–112 × 28–35
uterus L × W	—	260–312 (283) × 62–166 (110)	—	270–350 × 84–98
eggs L × W		21–33 (27) × 7–12 (9)		31–35 × 10–13

[a]range (mean) in micrometres except when otherwise noted.
[b]figures shown in boldface type are of structures not measured in the original description.

Fig. 1. Scanning electron microscopy images of adult specimens of *Microsentis wardae* from the posterior gut of *Gillichthys mirabilis* collected in the salty marches of Anaheim Bay, California. A whole female specimen showing the relative size and shape of the spheroidal proboscis, neck and the conical trunk.

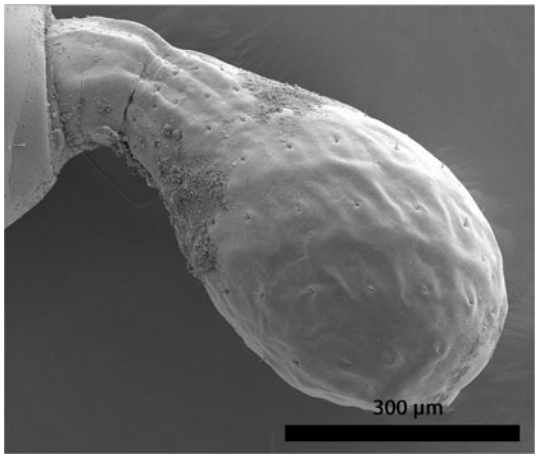

Fig. 2. Scanning electron microscopy images of adult specimens of *Microsentis wardae* from the posterior gut of *Gillichthys mirabilis* collected in the salty marches of Anaheim Bay, California. A pear-shaped proboscis and ventrally angulating neck.

close to edge of the hook base is attributed to the proximity of the exterior shell to the centre core. EDXA of the whole hook showed unusually highest level of sodium (table 2). It is worth noting that the reported WT% numbers should not be interpreted as compositional. They are, however, indicative of relative differences observed between the selected areas.

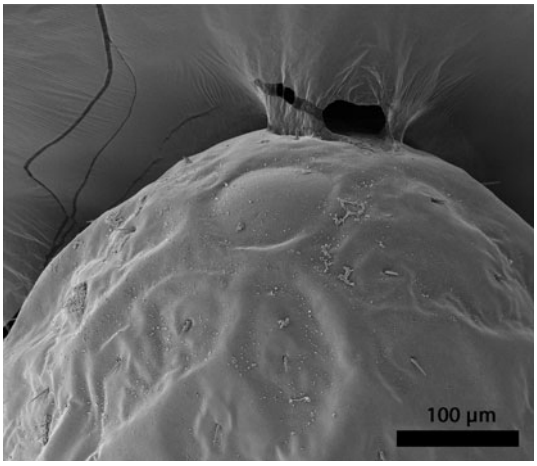

Fig. 3. Scanning electron microscopy images of adult specimens of *Microsentis wardae* from the posterior gut of *Gillichthys mirabilis* collected in the salty marches of Anaheim Bay, California. A view of the anterior proboscis showing the apical disc of the apical organ.

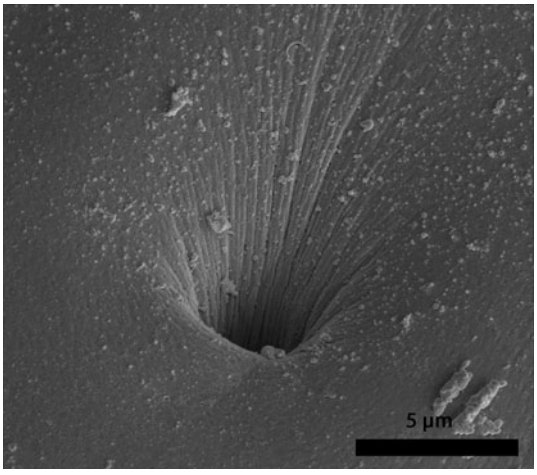

Fig. 4. Scanning electron microscopy images of adult specimens of *Microsentis wardae* from the posterior gut of *Gillichthys mirabilis* collected in the salty marches of Anaheim Bay, California. A sensory pore at the anterior proboscis.

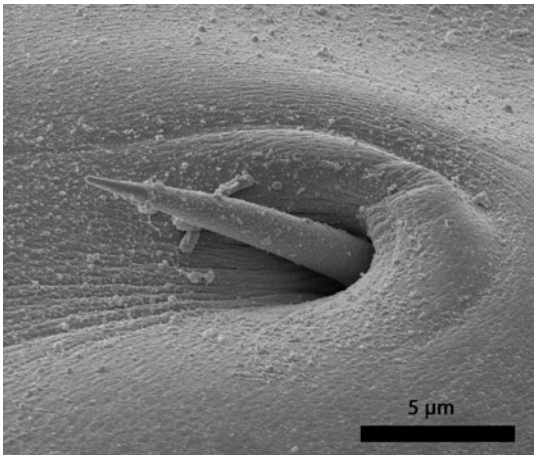

Fig. 5. Scanning electron microscopy images of adult specimens of *Microsentis wardae* from the posterior gut of *Gillichthys mirabilis* collected in the salty marches of Anaheim Bay, California. An apical hook. Note the epicuticular orifice at its point of insertion.

https://doi.org/10.1017/S0022149X22000347 Published online by Cambridge University Press

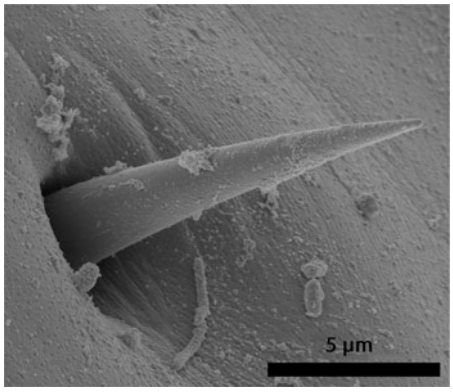

Fig. 6. Scanning electron microscopy images of adult specimens of *Microsentis wardae* from the posterior gut of *Gillichthys mirabilis* collected in the salty marches of Anaheim Bay, California. Image of a middle hook.

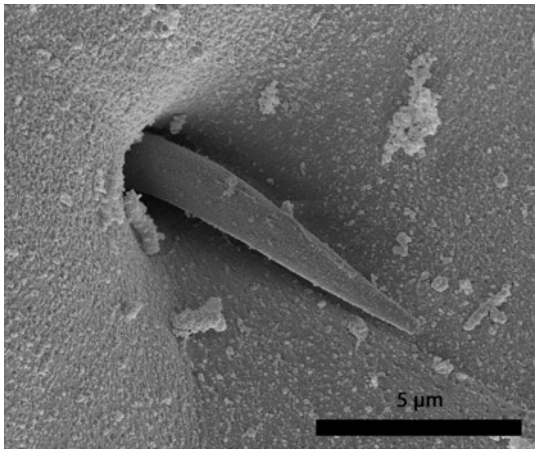

Fig. 7. Scanning electron microscopy images of adult specimens of *Microsentis wardae* from the posterior gut of *Gillichthys mirabilis* collected in the salty marches of Anaheim Bay, California. Image of a posterior hook.

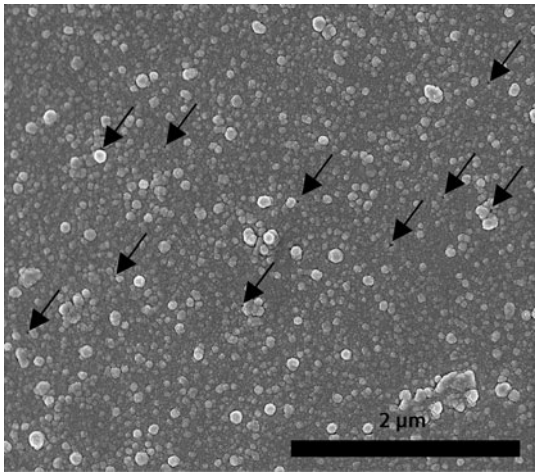

Fig. 8. Scanning electron microscopy images of adult specimens of *Microsentis wardae* from the posterior gut of *Gillichthys mirabilis* collected in the salty marches of Anaheim Bay, California. A few scattered micropores in the body wall of a female specimen (arrows).

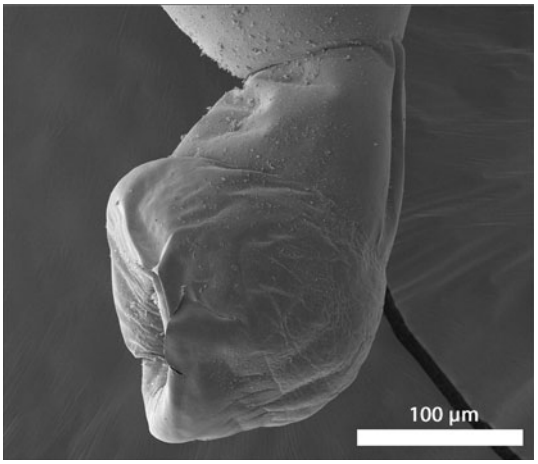

Fig. 9. Scanning electron microscopy images of adult specimens of *Microsentis wardae* from the posterior gut of *Gillichthys mirabilis* collected in the salty marches of Anaheim Bay, California. Lateral view of the bursa.

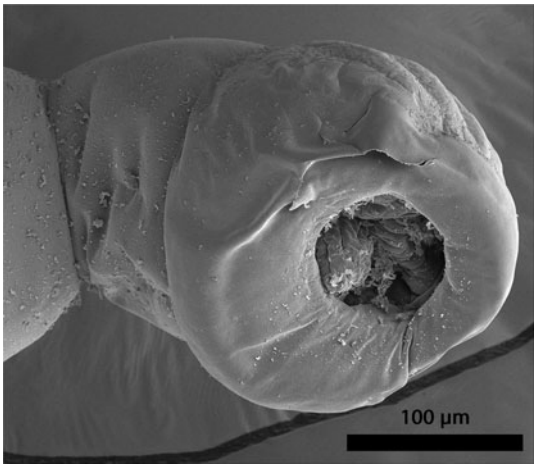

Fig. 10. Scanning electron microscopy images of adult specimens of *Microsentis wardae* from the posterior gut of *Gillichthys mirabilis* collected in the salty marches of Anaheim Bay, California. Ventral view of the bursa.

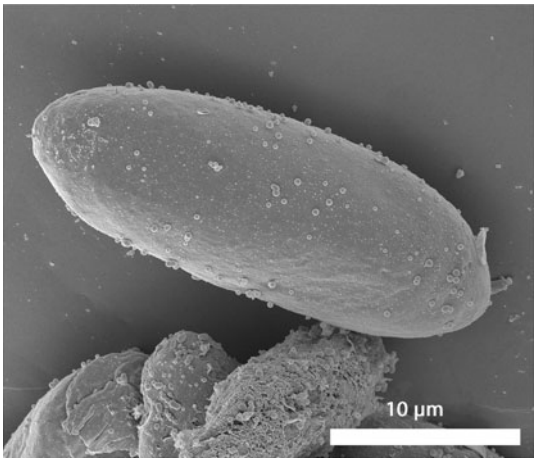

Fig. 11. Scanning electron microscopy images of adult specimens of *Microsentis wardae* from the posterior gut of *Gillichthys mirabilis* collected in the salty marches of Anaheim Bay, California. A mature egg. Note the absence of surface corrugations or fibrillar topography.

https://doi.org/10.1017/S0022149X22000347 Published online by Cambridge University Press

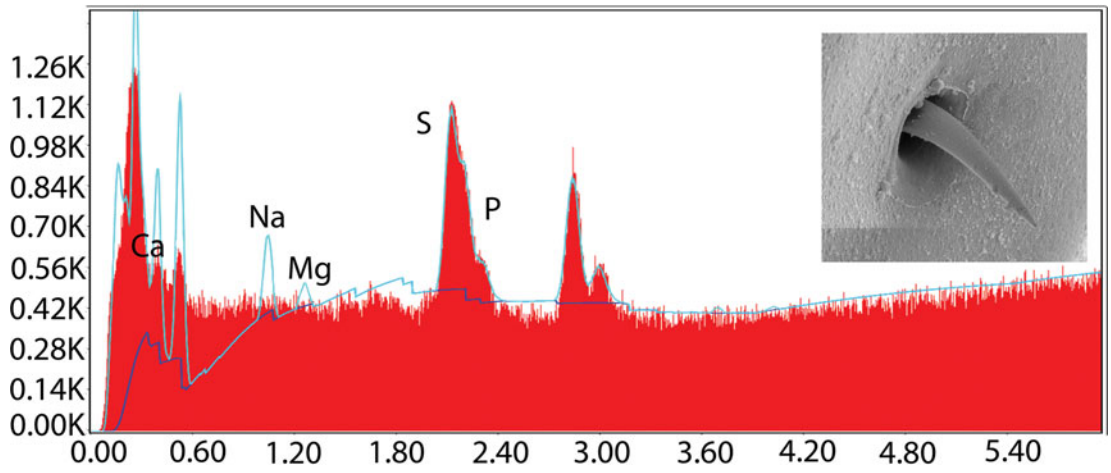

Fig. 12. X-ray panels of elemental scans of *Microsentis wardae* hooks. See table 2 for percentage weight of depicted elements. In all figures 12–14, the tallest peak to the far left is carbon and the 2 adjacent unlabelled peaks to the far right are palladium and gold. Scan of whole middle hook. Note the high level of sodium and sulphur compared to the lower levels of phosphorous, magnesium and calcium. Inset: whole middle hook.

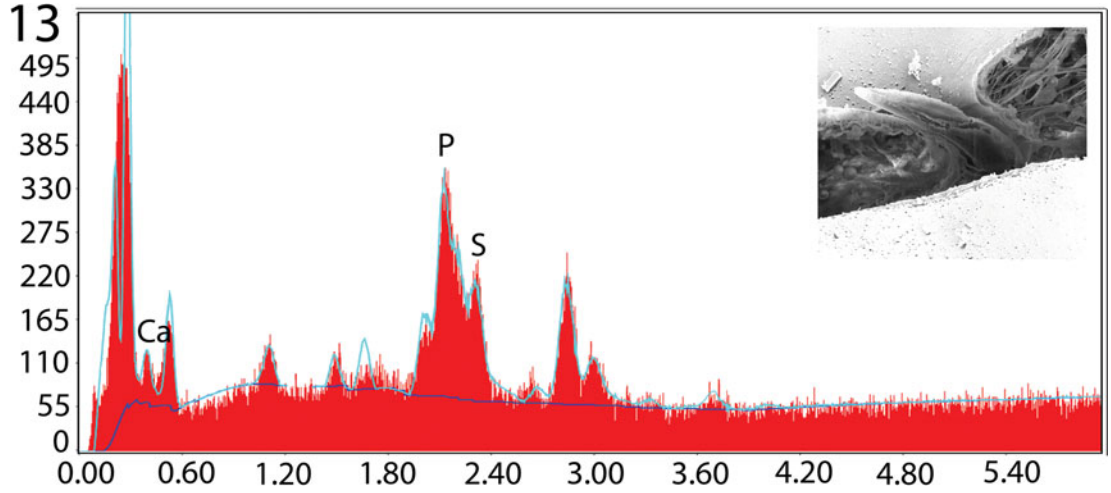

Fig. 13. X-ray panels of elemental scans of *Microsentis wardae* hooks. See table 2 for percentage weight of depicted elements. In all figures 12–14, the tallest peak to the far left is carbon and the 2 adjacent unlabelled peaks to the far right are palladium and gold. Scan of a longitudinal section of middle hook. Note the highest levels of sulphur and phosphorus in multiple specimens and the moderate level of calcium. Insert: longitudinal section of a middle hook.

Molecular results

The 18S data set of *M. wardae* included sequences from four isolates with 880–887 base pairs that show no intraspecific sequence divergence. Table 3 provides data for the sequences used from GenBank for the reconstruction of phylogenetic analyses. For the 18S gene, both ML and BI algorithms produced trees with identical topology (fig. 15). The 18S phylogenetic tree inferred from ML and BI analyses shows that the sequences of isolates of *M. warade* obtained is closely associated with a clade formed by species of the family Neoechinorhynchidae, that is, *Neoechinorhynchus* spp., *Hebesoma violentum* and *Floridosentis mugilis* (fig. 15). The sister relationships with the above species of acanthocephalans with *M. wardae* received strong bootstrap support (99%) and Bayesian posterior probabilities (1.0). Four sequences of *M. wardae* were strongly supported (100% ML and 1.00 BI) and remained clusters into a distinct clade (fig. 15). In both analyses, nevertheless, species of Neoechinorhynchidae are nested together which removes any inconsistencies and confirmed the status of this monotypic genus *Microsentis* with species *M. wardae* under Neoechinorhynchidae (fig. 15), which is also in accordance with the previous studies (Amin, 2013). Genetic divergence among the newly generated *M. wardae* sequences with *Neoechinorhynchus* spp. ranged 0.058–0.082% (36–50 nt difference), 0.122% (79 nt difference) with *H. violentum*, and 0.075 (45 nt difference) with *F. mugilis*, respectively.

Discussion

Morphology

The original assignment of the genus *Microsentis* was made to the neoechinorhynchid subfamily Tenuisentinae, now Family Tenuisentidae Van Cleave, 1936, but was later reassigned to Neoechinorhynchinae (Ward, 1917) Travassos, 1926. The morphometric findings of *M. wardae* from the same host species and locality quantified in table 1 show an extreme case of intraspecific morphological variations especially in trunk size and

https://doi.org/10.1017/S0022149X22000347 Published online by Cambridge University Press

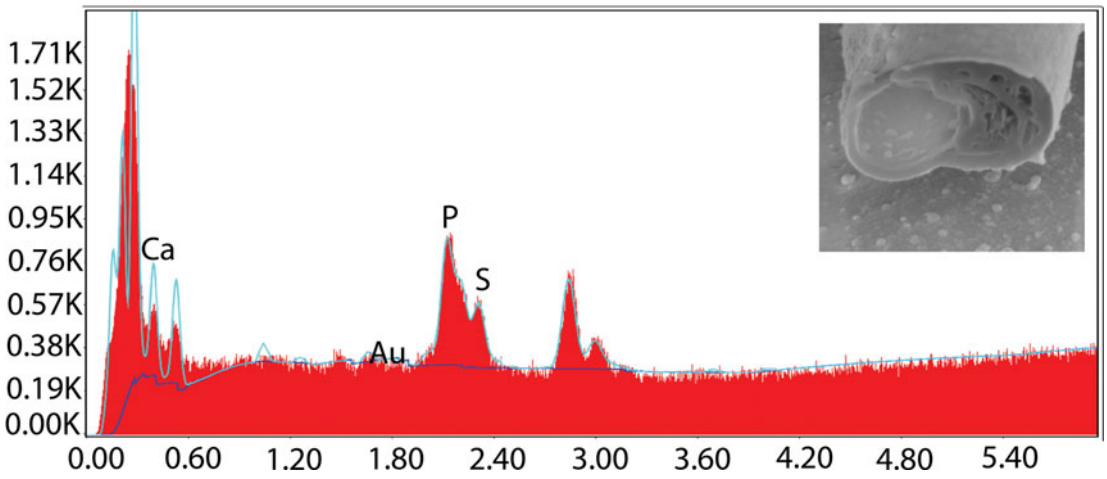

Fig. 14. X-ray panels of elemental scans of *Microsentis wardae* hooks. See table 2 for percentage weight of depicted elements. In all figures 12–14, the tallest peak to the far left is carbon and the 2 adjacent unlabelled peaks to the far right are palladium and gold. Scan of a cross-section of middle hook. Note the highest level of sulphur and phosphorous and the low level of all other elements. Insert: cross-section of a middle hook.

Table 2. The chemical composition of middle hooks of *Microsentis wardae* from *Gillichthys mirabilis* in California.

Element[a]	Whole hook	Longitudinal section	Cross-section
magnesium	1.32	0.10–0.24	0.32
sodium)	5.47	0.22–0.29	1.21
phosphorous	0.02	3.31–6.59	0.80
sulphur	2.61	6.08–6.38	4.70
calcium	1.09	1.97–3.12	0.58

[a]palladium and gold were used to count the specimens and the gallium for the cross cut of the hooks. These and other elements (carbon, oxygen and nitrogen) common in organic matter are omitted. Data are reported in weight (WT%) and demonstrated in three spectra (figs 12 and 13).

proportion of the size of proboscis and the receptacle to trunk size. We observed one worm with a calcareous collar similar to that shown by Martin & Multani (1966, fig. 3). Our specimens were sexually mature and females as small as 1.57 mm had fully ripe eggs. Martin & Multani (1966; p. 537) reported females reaching 5.00 mm long but a female as small as 0.98 mm long contained ovarian balls and another 1.3 mm long female contained eggs. Martin & Multani's (1966) 'measurements were taken mainly of living material (p. 536) and hence are greater than would be obtained solely of fixed material.' They also reported that 'both sexes continue to grow after reaching sexual maturity.' Size differences are related to different rates of growth and development. And since, in acanthocephalans, growth does not occur at the same rate in different body parts, one ends up with different ratios. In *M. wardae*, the trunk grows at a slower rate than the proboscis and the receptacle later in development. Our worms were younger than those described by Martin & Multani (1966) and somatic development priorities appear to be devoted to attachment structures first, to ensure efficient attachment to host gut after recruitment. A similar initial surge of proboscis and receptacle growth was observed in juveniles of other acanthocephalan species including *Neoechinorhynchus cylindratus* (Van Cleave, 1913) Van Cleave (1919) from *Micropterus salmoides* (Lacépède) in Wisconsin (Amin, 1986). Differential growth rates have been observed in other species of acanthocephalans especially dorsally vs. ventrally causing the translocation of female gonopore from terminal in immatures to sub-ventral in more mature adults. Examples: see Amin & Heckmann (1992) on *Neoechinorhynchus idahoensis* Amin & Heckmann, 1992; and Amin & Bullock (1998) on *N. cylindratus*.

We noted usually six giant nuclei in the cement glands but eight were occasionally observed. Martin & Multani (1966) reported eight giant nuclei and papillae on each side of the penis that were barely visible in our microscopical observations. Our SEM images of the bursa (figs 9 and 10) show only external features.

Micropores

The micropores of *M. wardae* are associated with internal crypts and vary in diameter and distribution in different trunk regions corresponding with differential absorption of nutrients. We have reported micropores in a large number of acanthocephalan species (Heckmann *et al.*, 2013) and in a few more since, and demonstrated the tunnelling from the cuticular surface into the internal crypts by transmission electron microscopy in *Corynosoma strumosum* (Rudolphi, 1802) Lühe, 1904 from the Caspian seal *Pusa caspica* (Gmelin) in the Caspian Sea (figs 19 and 20 of Amin *et al.*, 2011) and in *Neoechinorhynchus personatus* Tkach, Sarabeev, Shvetsova, 2014 from *Mugil cephalus* Linn. in Tunisia (figs 26, 29 and 30 in Amin *et al.*, 2020); Amin *et al.* (2009) gave a summary of the structural–functional relationship of the micropores in various acanthocephalan species. Wright & Lumsden (1969) and Byram & Fisher (1973) reported that the peripheral canals of the micropores are continuous with canalicular crypts constituting a huge increase in external surface area … implicated in nutrient up take. Whitfield (1979) estimated a 44-fold increase at a surface density of 15 invaginations per 1 μm² of *Moniliformis moniliformis* tegumental surface.

EDXA

Our studies of acanthocephalan worms have usually involved X-ray scans (EDXA) of FIB-sectioned hooks and spines (Heckmann *et al.*, 2007, 2012b; Standing & Heckmann, 2014). Hooks and

https://doi.org/10.1017/S0022149X22000347 Published online by Cambridge University Press

Table 3. Acanthocephalan species information used for phylogenetic analysis based on the 18S gene sequences. NA = not available.

Species	Host	Host origin	GenBank accession numbers	References
Acanthosentis Verma and Datta 1929				
Acanthosentis kashmirensis	*Schizothorax plagiostomus*	India	MW000900	Sharifdini *et al.*, 2021
Acanthosentis fusiformis	*Arius* sp.	Vietnam	MK834518	Amin *et al.*, 2019c
Floridosentis Ward 1953				
Floridosentis mugilis	*Mugil cephalus*	Mexico	AF064811	García-Varela *et al.*, 2000
Hebesoma Van Cleave 1928				
Hebesoma violentum	*Perccottus glenii*	Russia	KF156881	Malyarchuk *et al.*, 2014
Microsentis Martin & Multani, 1966				
Microsentis wardae	*Gillichthys mirabilis*	Unites States	OM831948	this study
			OM831949	
			OM831950	
			OM831951	
Neoechinorhynchus Stiles and Hassall 1905				
Neoechinorhynchus qinghaiensis	NA	China	MW144440	Pan, 2020*
Neoechinorhynchus sp.	NA	China	KM507363	Liu *et al.* 2014*
Neoechinorhynchus sp.	*Capoeta aculeata*	Iran	KU363972	Dadar & Adel, 2016*
Neoechinorhynchus crassus	NA	Unites States	AF001842	Near *et al.*, 1998
N. crassus	NA	Iran	KU363969	Dadar & Adel, 2016*
Neoechinorhynchus pseudemydis	NA	United States	NPU41400	Near & Nadler, 1996*
Neoechinorhynchus cylindratus	*Micropterus salmoides*	Unites States	MF974925	Blubaugh & Gauthier, 2018*
Neoechinorhynchus saginata	NA	United States	AY830150	García-Varela & Nadler, 2005
Neoechinorhynchus buttnerae	NA	Brazil	MW590330	Soares *et al.* 2021*
N. buttnerae	NA	Brazil	MK249749	Souza and Benavides, 2018*
Outgroup				
Leptorhynchoides thecatus	NA	United States	AF001840	Near *et al.*, 1998
Mediorhynchus sp.	NA	Mexico	AF064816	García-Varela *et al.*, 2000
Moniliformis cryptosaudi	*Hemiechinus auritus*	Iraq	MH401043	Amin *et al.*, 2019b
Macracanthorhynchus hirudinaceus	*Sus scrofa leucomystax*	Japan	LC350002	Kamimura *et al.*, 2018

*, shows the unpublished status of a species on GenBank database.

spines are evaluated for chemical ions with sulphur, calcium and phosphorus being the prominent elements. Sulphur is usually seen at the outer edge of large hooks and calcium and phosphorus are major ions in the base and middle of hooks where tension and strength are paramount for hook function. Sodium, a rarely prominent metal, was most prominent in scans of whole hooks of *M. wardae* (table 2, fig. 12). It was also prominent in whole hooks of *Pallisentis nandai* Sarkar, 1953 (see Amin *et al.*, 2021) as well as in egg shells of *Neoechinorhynchus qatarensis* Amin, Saoud, Alkuwari, 2002 (see Heckmann *et al.*, 2007). 'The absence of sodium at the hook tip and its presence at the hook base and the opposite pattern of sulfur are characteristic of *Neoechinorhynchus dimorphospinus* Amin and Sey, 1996 hooks' (Amin *et al.*, 2019a, p. 616).

Results of the X-ray analysis of the FIB-sectioned hooks (dual beam SEM) of *M. wardae* show differential composition and distribution of metals in different hook parts characteristic of that species. Whole hooks and sections showed the highest level of sulphur and lowest levels of calcium and phosphorus (table 2). *Cavisoma magnum* (Southwell, 1927) Van Cleave, 1931 from *Mugil cephalus* in the Arabian Sea, has a similar pattern but considerably higher levels of sulphur in hook tips (43.51 WT%) and edges (27.46 WT%) (Amin *et al.*, 2018). This element (sulphur) is part of the prominent outer layer of most acanthocephalan hooks and is a major contributor of the hardening process of hooks. Our results are comparable to those of mammalian teeth enamel. The EDXA appears to be species-specific, as in fingerprints. For example, *Moniliformis cryptosaudi* Amin, Heckmann, Sharifdini, Albayati, 2019 from Iraq is morphologically identical to *Moniliformis saudi* Amin, Heckmann, Mohammed, Evans, 2016 from Saudi Arabia, and it was erected based primarily on its distinctly different EDXA pattern (Amin *et al.*, 2019b) as a cryptic species. Our methodology for the detection of the chemical profile of hooks in the Acanthocephala has also been used in other parasitic groups including the Monogenea (Rubtsova *et al.*, 2018; Rubtsova & Heckmann, 2019) and Cestoda (Rubtsova & Heckmann, 2020).

https://doi.org/10.1017/S0022149X22000347 Published online by Cambridge University Press

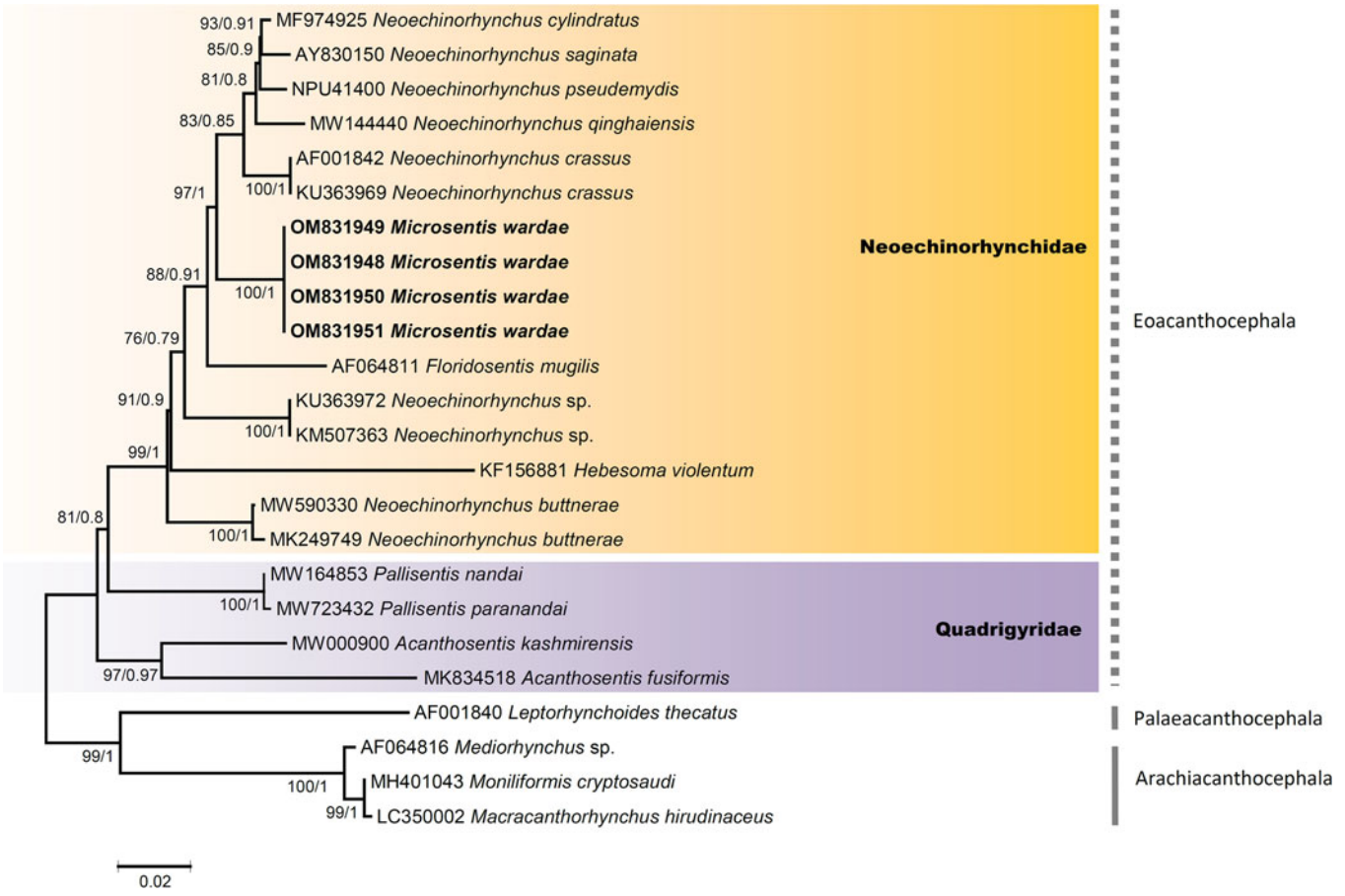

Fig. 15. Phylogenetic reconstruction using 18S rDNA sequences of *Microsentis wardae* (shown in boldface type) and sequences of Acanthocephala deposited in the GenBank. The numbers indicate values of bootstrap >75%. Numbers above branches indicate nodal support as maximum likelihood and posterior probabilities from Bayesian inference. Species of Arachiacanthocephala and Palaeacanthocephala are used as an outgroup. The scale-bar indicates the expected number of substitutions per site.

The biological significance of EDXA as a diagnostic tool is exemplified by the observation that populations of an acanthocephalan species will consistently have similar EDXA spectra irrespective of host species or geography, even though comparative morphometrics of different populations of the same species usually vary with host species and geography; see, for example, Amin & Redlin (1980) and Amin & Dailey (1998). The taxonomic identity of species is deep-seated at the genetic level manifesting the organism's morphology and biochemistry as revealed, in part, by its elemental spectra. In discussing the EDXA of *N. personatus* Tkach, Sarabeev, Shvetsova, 2014 from *M. cephalus* Linn., Amin *et al.* (2020) noted that 'The anterior and posterior hooks of our *N. personatus* in the Mediterranean and Black Sea had comparable biochemical profiles'. Metal analysis of hooks has become a diagnostic standard since hooks have the highest level of elements compared to the mid- and posterior trunk regions of the acanthocephalan body (Heckmann *et al.* 2012a). Specifically, the sulphur content in the proboscis is paramount in the composition of disulphide bonds in the thiol groups for cysteine and cystine of the polymerized protein molecules (Stegman, 2005). Protein synthesis occurs in two stages, transcription and translation, by transferring of genetic instructions in the nuclear DNA to mRNA in the ribosomes followed by post-translational events such as protein folding and proteolysis (Stegman, 2005). The formed disulphide bonds are direct by-products of the DNA-based process of protein synthesis which makes up the identity of a biological species. Accordingly, the level of sulphur, in our EDXA profiles, will indicate the number of sulphur bonds that along with the levels of calcium phosphates, will characterize the identity of a species based on its nuclear DNA personality. Differences in chemical compositions probably indicate differences in allele expression. The DNA generated sulphide bonds evident in our EDXA profiles have an important role in the stability and rigid nature of the protein accounting for the high sulphur content of the proboscis (Heckmann *et al.*, 2012a). The above processes explain the observed species-specific nature of EDXA profiles noted in our many findings.

Molecular analysis

To date, no genetic data have been provided for this monotypic genus *Microsentis* Martin & Multani, 1966 with species *M. wardae*. Lack of molecular data creates difficulties for determining relationships among members of other genera and their taxonomic position. We add new molecular data for *M. wardae* inferred from the 18S ribosomal gene for the first time. The 18S analysis reliably showed that the species *M. wardae* forms a strongly supported clade with members of the family Neochinorhynchidae. This relationship was morphologically established previously and *M. wardae* was assigned to the Neochinorhynchidae (Amin, 2013), which is also supported

https://doi.org/10.1017/S0022149X22000347 Published online by Cambridge University Press

by the present study. Here in the tree, the presence of a single clade for four isolates of *M. wardae* from the United States was confirmed but the distribution pattern based on the genetic data will be confirmed after including a number of isolates of *M. wardae* from different regions and hosts to better understand the evolutionary relationships among the order Neoechinorhynchida. Regarding the phyletic assemblage of the genus *Neoechinorhynchus* species present in the phylogenetic tree (fig. 15), we found that the sequences were not construed as a monophyletic assemblage in the18S analysis. The genus *Neoechinorhynchus* requires a taxonomic revision.

To summarize, we suggest that the morphological description of acanthocephalan diversity necessitates the use of molecular data. Sequences from species of other genera of the Neoechinorhynchidae emphasize the importance of revealing relationships within the Eoacanthocephala in future studies.

Acknowledgements. The energy dispersive X-ray analysis and scanning electron microscopy methodologies used in this project have been pioneered by Dr Richard A. Heckmann (deceased) (Brigham Young University (BYU)) to whom we shall always dedicate our highest gratitude. We thank Madison Laurence, Bean Museum (BYU) for expert help in the preparation and organization of plates and figures and Michael Standing, Electron Optics Laboratory (BYU), for his technical help and expertise. We acknowledge the laboratory facilities provided by the Department of Zoology, Chaudhary Charan Singh University, Meerut, India. We are also very grateful to Dr. Ralph Appy, Cabrillo Marine Aquarium, San Pedro, California for providing the specimens of M. wardae used in this study.

Financial support. This project was supported by the Department of Biology, Brigham Young University, Provo, Utah, and by an Institutional Grant from the Parasitology Center, Inc, Scottsdale, Arizona.

Conflict of interest. None.

Ethical approval. The authors declare that they have observed all applicable ethical standards.

References

Amin OM (1986) Acanthocephala from lake fishes in Wisconsin: Morphometric growth of *Neoechinorhynchus cylindratus* (Neoechinorhynchidae) and taxonomic implications. *Transactions of the American Microscopical Society* **105(4)**, 375–380.

Amin OM (2013) Classification of the acanthocephala. *Folia Parasitol* **60(4)**, 273–305.

Amin OM and Bullock WL (1998) *Neoechinorhynchus rostratum* sp. n. (Acanthocephala: Neoechinorhynchidae) from the eel, *Anguilla rostrata*, in estuarine waters of northeastern North America. *Journal of the Helminthological Society of Washington* **65(2)**, 169–173.

Amin OM and Dailey MD (1998) Description of *Mediorhynchus papillosus* (Acanthocephala: Gigantorhynchidae) from a Colorado, U.S.A., population, with a discussion of morphology and geographical variability. *Journal of Helminthological Society of Washington* **65(2)**, 189–200.

Amin OM and Heckmann RA (1992) Description and pathology of *Neoechinorhynchus idahoensis* n. sp. (Acanthocephala: Neoechinorhynchidae) in *Catostomus coumbianus* from Idaho. *Journal of Parasitology* **78(1)**, 34–39.

Amin OM and Redlin MJ (1980) The effect of host species on growth and variability of *Echinorhynchus salmonis* Müller, 1784 (Acanthocephala: Echinorhynchidae), with special reference to the status of the genus. *Systematic Parasitology* **2(1)**, 9–20.

Amin OM, Heckmann RA, Radwan NA, Mantuano JS and Alcivar MAZ (2009) Redescription of *Rhadinorhynchus ornatus* (Acanthocephala: Rhadinorhynchidae) from skipjack tuna, *Katsuwonus pelamis*, collected in the Pacific Ocean off South America, with special reference to new morphological features. *Journal of Parasitology* **95(3)**, 656–664.

Amin OM, Heckmann RA, Halajian A and El-Naggar AM (2011) The morphology of an [sic] unique population of *Corynosoma strumosum* (Acanthocephala, Polymorphidae) from the Caspian seal, *Pusa caspica*, in the land-locked Caspian Sea using SEM, with special notes on histopathology. *Acta Parasitologica* **56(4)**, 438–445.

Amin OM, Heckmann RA and Bannai MA (2018) *Cavisoma magnum* (Cavisomidae), a unique Pacific acanthocephalan redescribed from an unusual host, *Mugil cephalus* (Mugilidae), in the Arabian Gulf, with notes on histopathology and metal analysis. *Parasite* **25**, 5.

Amin OM, Sharifdini M, Heckmann RA and Ha NV (2019a) On three species of *Neoechinorhynchus* (Acanthocephala: Neoechinorhynchidae) from the Pacific Ocean off Vietnam with the molecular description of *Neoechinorhynchus* (*N.*) *dimorphospinus* Amin and Sey, 1996. *Journal of Parasitology* **105(4)**, 606–618.

Amin OM, Heckmann RA, Sharifdini M and Albayati NY (2019b) *Moniliformis cryptosaudi* n. sp. (Acanthocephala: Moniliformidae) from the Long-eared Hedgehog *Hemiechinus auritus* (Gmelin) (Erinaceidae) in Iraq; A Case of Incipient Cryptic Speciation Related to *M. saudi* in Saudi Arabia. *Acta Parasitologica* **64(1)**, 195–204.

Amin OM, Chaudhary A, Heckmann RA, Ha NV and Singh HS (2019c) The morphological and molecular description of *Acanthogyrus* (*Acanthosentis*) *fusiformis* n. sp. (Acanthocephala: Quadrigyridae) from the catfish *Arius* sp. (Ariidae) in the Pacific Ocean off Vietnam, with notes on zoogeography. *Acta Parasitologica* **64(4)**, 779–796.

Amin OM, Sharifdini M, Heckmann RA, Rubtsova N and Chine HJ (2020) On the *Neoechinorhynchus agilis* (Acanthocephala: Neoechinorhynchidae) complex, with the description of *Neoechinorhynchus ponticus* n. sp. from *Chelon auratus* Risso in the Black Sea. *Parasite* **27**, 48.

Amin OM, Heckmann RA, Chaudhary A, Rubtsova NY and Singh HS (2021) Redescription and molecular analysis of *Pallisentis* (*Pallisentis*) *nandai* Sarkar, 1953 (Acanthocephala: Quadrigyridae) in India. *Journal of Helminthology* **95**, e3.

Anonymous (2009) Sedimentology and Oceanography of Coastal Lagoons in Baja California, Mexico—Geological Society of America Bulletin. Available at gsabulletin.gsapubs.org (accessed 1 November 2009).

Byram JE and Fisher Jr FM (1973) The absorptive surface of *Moniliformis dubius* (Acanthocephala). 1. Fine structure. *Tissue and Cell* **5(4)**, 553–579.

Eschmeyer WN, Herald ES and Hamann H (1983) *A field guide to pacific coast fishes of North America. Peterson field guide series*. Boston, MA, Houghton Mifflin Co.

García-Prieto L, García-Varela M, Mendoza-Garfias B and Pérez-Ponce de León G (2010) Checklist of the Acanthocephala in wildlife vertebrates of Mexico. *Zootaxa* **2419**, 1–50.

García-Varela M and Nadler SA (2005) Phylogenetic relationships of Palaeacanthocephala (Acanthocephala) inferred from SSU and LSU rDNA gene sequences. *Journal of Parasitology* **91(6)**, 1401–1409.

García-Varela M, Pérez-Ponce de León G, de la Torre P, Cummings MP, Sarma SS and Laclette JP (2000) Phylogenetic relationships of Acanthocephala based on analysis of 18S ribosomal RNA gene sequences. *Journal of Molecular Evolution* **50(6)**, 532–540.

García E (2018) *Genomic analysis of disjunct marine fish populations of the northeastern Pacific and Sea of Cortez*. Thesis, UC Santa Cruz

Heckmann RA, Amin OM and Standing MD (2007) Chemical analysis of metals in acanthocephalans using energy dispersive X-ray analysis (EDXA, XEDS) in conjunction with a scanning electron microscope (SEM). *Comparative Parasitology* **74(2)**, 388–391.

Heckmann RA, Amin OM, Radwan NAE, Standing MD and Eggett DL (2012a) Comparative chemical element analysis using energy dispersive x-ray microanalysis (EDXA) for four species of Acanthocephala. *Scientia Parasitologica* **13**, 27–35.

Heckmann RA, Amin OM, Radwan NAE, Standing MD, Eggett DL and El Naggar AM (2012b) Fine structure and energy dispersive X-ray analysis (EDXA) of the proboscis hooks of *Radinorynchus ornatus*, Van Cleave 1918 (Rhadinorynchidae: Acanthocephala). *Scientia Parasitologica* **13(1)**, 37–43.

Heckmann RA, Amin OM and El Naggar AM (2013) Micropores of Acanthocephala, a scanning electron microscopy study. *Scientia Parasitologica* **14(3)**, 105–113.

Kamimura K, Yonemitsu K, Maeda K, Sakaguchi S, Setsuda A, Varcasia A and Sato H (2018) An unexpected case of a Japanese wild boar (*Sus*

https://doi.org/10.1017/S0022149X22000347 Published online by Cambridge University Press

scrofa leucomystax) infected with the giant thorny-headed worm (*Macracanthorhynchus hirudinaceus*) on the mainland of Japan (Honshu). *Parasitology Research* **117(7)**, 2315–2322.

Lee R (1992) *Scanning electron microscopy and X-ray microanalysis*. Englewood Cliffs, New Jersey, Prentice Hall, p. 464.

Malyarchuk B, Derenko M, Mikhailova E and Denisova G (2014) Phylogenetic relationships among *Neoechinorhynchus* species (Acanthocephala: Neoechinorhynchidae) from North-East Asia based on molecular data. *Parasitology International* **63(1)**, 100–107.

Martin WE and Multani S (1966) *Microsentis wardae* n. g., n. sp. (Acanthocephala) in the marine fish *Gillichthys mirabilis* Cooper. *Transactions of the American Microscopical Society* **85(4)**, 536–540.

Martin WE and Multani S (1970) Some helminths of the mudsucker fish, *Gillichthys mirabilis* Cooper. *Bulletin of the Society of the California Academy of Sciences* **69(1)**, 161–168.

Milne I, Lindner D, Bayer M, Husmeier D, Mcguire G, Marshall DF and Wright F (2009) TOPALiv2: A rich graphical interface for evolutionary analyses of multiple alignments on HPC clusters and multi-core desktops. *Bioinformatics* **25(1)**, 126–127.

Near TJ, Garey JR and Nadler SA (1998) Phylogenetic relationships of the Acanthocephala inferred from 18S ribosomal DNA sequences. *Molecular Phylogenetics and Evolution* **10(3)**, 287–298.

Phleger FB and Clifford CE (2009) Ewing. "Protected Areas Programme - Whale Sanctuary of El Vizcaino". Available at www.unep-wcmc.org (accessed 1 November 2009).

Posada D (2008) jModelTest: phylogenetic model averaging. *Molecular Biology and Evolution* **25(7)**, 1253–1256.

Rubtsova NY and Heckmann RA (2019) Structure and morphometrics of *Ancyrocephalus paradoxus* (Monogenea: Ancyrocephalidae) from *Sander lucioperca* (Percidae) in Czechia. *Helminthologia* **56(1)**, 11–21.

Rubtsova NY and Heckmann RA (2020) Morphological features and structural analysis of plerocercoids of *Spirometra erinaceieuropaei* (Cestoda: Diphyllobothriidae) from European pine marten, *Martes martes* (Mammalia: Mustelidae) in Ukraine. *Comparative Parasitology* **87(1)**, 109–117.

Rubtsova NY, Heckmann RA, Smit WS, Luus-Powell WJ, Halajian A and Roux F (2018) Morphological studies of developmental stages of *Oculotrema hippopotami* (Monogenea: Polystomatidae) infecting the eye of *Hippopotamus amphibius* (Mammalia: Hippopotamidae) using SEM and EDXA with notes on histopathology. *Korean Journal of Parasitology* **56(5)**, 463–475.

Sharifdini M, Amin OM and Heckmann RA (2021) The molecular profile of *Acanthogyrus* (*Acanthosentis*) *kashmirensis* from the Indian subcontinent. *Acta Parasitologica* **66(3)**, 863–870.

Standing MD and Heckmann RA (2014) Features of Acanthocephalan hooks using dual beam preparation and XEDS phase maps. *Microscopy and Microanalysis Meeting*, Hartford, Connecticut, USA, No 0383–00501.

Stegman JK (2005) *Stedman's Medical Dictionary for health professions and Nursing*. 5th Edition. Baltimore, Maryland, USA, Lippincott, Williams and Wilkins.

Suzuki N, Hoshino K, Murakami K, Takeyama H and Chow S (2008) Molecular diet analysis of *Phyllosoma* larvae of the Japanese spiny lobster *Palinurus japonicas* (Decapoda: Crustacea). *Marine Biotechnology* **10(1)**, 49–55.

Tamura K, Stecher G and Kumar S (2021) MEGA11: Molecular Evolutionary Genetics Analysis Version 11. *Molecular Biology and Evolution* **38(7)**, 3022–3027.

Thompson JD, Gibson TJ, Plewniak F, Jeanmougin F and Higgins DG (1997) The CLUSTAL_X windows interface: flexible strategies for multiple sequence alignment aided by quality analysis tools. *Nucleic Acids Research* **25(24)**, 4876–4882.

Whitfield PJ (1979) *The biology of parasitism: an introduction to the study of associating organisms*. Baltimore, Maryland, University Park Press, p. 277.

Wright RD and Lumsden RD (1969) Ultrastructure of the tegumentary pore-canal system of the acanthocephalan *Moniliformis dubius*. *Journal of Parasitology* **55(5)**, 993–1003.

https://doi.org/10.1017/S0022149X22000347 Published online by Cambridge University Press